CHAPTER 5

ACTIVE ABSORPTION OF MULTIDIRECTIONAL WAVES

Hemming A. Schäffer[1)] and Jesper Skourup[2)]

Abstract

The development of a control system for active absorption of multidirectional waves is described. The present work is an extension of a two-dimensional flume system to include the wave propagation direction. The hydrodynamic feedback necessary for the active absorption is taken to be the surface elevation measured at each segment of the multidirectional wavemaker. A frequency-direction domain transfer function relating the paddle position to the measured and desired elevations is derived. For practical applications a two-dimensional digital filter is used for a time-space realization of the generation/absorption procedure. Experimental verification is made in a numerical wave tank using a Boundary Element Model. The numerical setup includes a moving boundary representing a segmented wavemaker. This ensures a realistic reproduction of evanescent wave modes, which can be important for the system performance. The numerical tests show that a quasi three-dimensional system consisting of an array of absorbing wavemakers developed for wave flumes is far better than having no active absorption. The present fully three-dimensional absorption system is shown to further reduce spurious reflections to around one third in the examples treated. Although the system is capable of simultaneous wave generation and active absorption, only the absorption ability was used in these preliminary tests.

1. Introduction

Spurious wave reflection remains an important problem in physical as well as numerical model testing of coastal and offshore structures. Open boundaries are often modelled by passive absorbers using e.g. physical perforated plates and numerical sponge layers. In numerical models the absorption performance is often poor for very oblique waves and unwanted diffraction into the sponge layer is a problem for waves travelling along such boundaries. In physical models spurious re-reflection from the wavemaker can lead to considerable distortion of the incident wave field or even to spurious resonance in the model.

[2)] International Research Centre for Computational Hydrodynamics (ICCH) at [1)] Danish Hydraulic Institute, Agern Allé 5, DK-2970 Hørsholm, Denmark

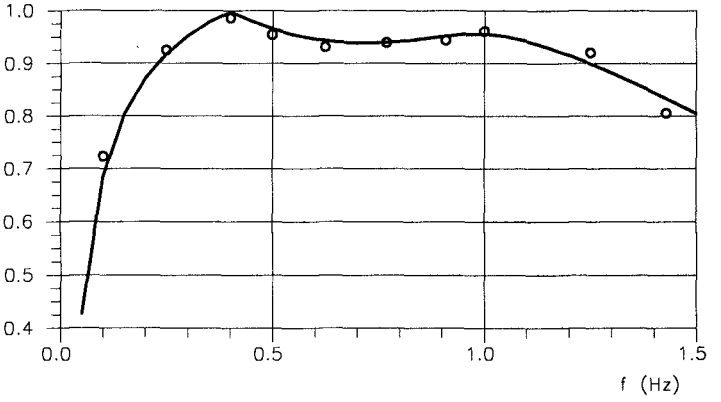

Figure 1 Absorption coefficients for active absorption tests in a numerical wave flume using 2D-AWACS. The full curve gives the theoretical performance. Water depth 1m.

This work primarily regards the problem of active absorption from a physical model point of view, but the system developed is also relevant for numerical modelling. The performance of the system is actually analysed using a numerical wave tank.

Recently, the original electric system used for active absorption in flumes at the Danish Hydraulic Institute was revised, leading to a digital Active Wave Absorption Control System called AWACS. The theoretical background and preliminary performance results are given in Schäffer et al. (1994). Since then, enhancements of the recursive filters involved have further improved the results. Applying the technique used in the AWACS, Skourup and Schäffer (1995) demonstrated that the absorption performance could be investigated using a numerical wave flume based on a Boundary Element Model (BEM). Figure 1 compares numerically determined absorption coefficients (found by analysing surface elevation time series from the numerical simulation) with theoretical values (given by the theory behind the active wave absorption system). Similar results were obtained from physical model tests and it appears that the BEM is well suited for a numerical test of an active absorption system for multidirectional waves, as pursued in this work.

The most simple way of introducing active absorption for a segmented multidirectional wavemaker is to apply a system developed for a wave flume to the control of each segment. This was done by e.g. Hirakuchi et al. (1992) using the flume system of Hirakuchi et al. (1990). However, this method only works well for weakly oblique waves. The trouble is that the system overreacts for oblique waves resulting in spurious wave generation.

When generating waves by the snake principle it is well known that for a fixed wave height, oblique waves require a smaller stroke than normally emitted waves. Specifically, the transfer function relating the wavemaker paddle stroke to the amplitude of the progressive wave is proportional to $\cos\theta$ where θ is the angle of emission (zero for normally emitted waves). Since active absorption is the reverse process of wave generation (i.e. reversing time), this $\cos\theta$ should also

be accounted for in the absorption of oblique waves. When the hydrodynamic feedback to the control system is taken as the elevation measured on the paddle front the presence of evanescent modes can be important. In this case the simple $\cos\theta$-variation of the involved transfer function is changed to a more complicated one which not only includes a θ-dependent amplitude but also a θ-dependent phase shift.

The flume AWACS has two inputs and one output. At each time step the inputs are the elevation of the desired incident waves and the elevation measured at the paddle of the wavemaker. The output is the position of the wavemaker paddle. The two inputs are combined in a simple manner reducing the system to a single-input-single-output system. For the multidirectional wave case a general multiple-input-multiple-output system is in principle required. The input represents desired incident waves and the hydrodynamic feedback, e.g. surface elevation measured on each paddle, and the output is the position of each paddle. Using a number of flume systems in parallel (which is the equivalent of making the approximation $\cos\theta = 1$) the multiple-input-multiple-output system is simplified to a number of parallel single-input-single-output systems. However, if $\theta \neq 0$ is to be accounted for, each paddle should at least be influenced by the hydrodynamic feedback at neighbouring flaps. Such a system is developed allowing for any number of directions to be represented at each frequency. Analysis of the system performance is made using the BEM to simulate the physical wave tank including the moving boundary representing the segmented wavemaker.

Since the 2D-AWACS is the basis for the present 3D system the next chapter gives a short review. In Chapter 3 the theory for multidirectional active wave absorption is derived and Chapter 4 gives some basic ideas for the practical inclusion of directional information. The general approach taken for the 3D-AWACS is shown in Chapter 5 and verification by experiments in a numerical wave tank is given in Chapter 6. Finally, summary and conclusions are presented in Chapter 7.

2. Review of the 2D-AWACS

The active wave absorption control system for wave flumes (2D-AWACS) presented by Schäffer et al. (1994) is based on a frequency domain expression for the wavemaker paddle position which may be formulated as

$$X_a = (2A_I - A_0)\,F_0; \qquad F_0 \equiv \frac{1}{i\sum_{j=0}^{\infty} c_j^*} \tag{1}$$

in which "*" denotes complex conjugation and i is the imaginary unit. Here A_I and A_0 are the complex amplitudes of the desired incident wave elevation and the elevation measured on the wave board. F_0 is a complex transfer function based on a real transfer function c_0 and some imaginary transfer functions c_j. Here c_0, which is sometimes called the Biésel transfer function, relates the amplitude of the generated wave to the amplitude of the paddle motion in the case of pure wave generation. The rest of the series in (1) is imaginary, and it relates the amplitude of the evanescent modes at the wave board to the amplitude of the paddle motion. For a piston type wavemaker we have

$$c_j = \frac{4\sinh^2 k_j h}{2k_j h + \sinh 2k_j h} \tag{2}$$

see e.g. Schäffer (1996) for results for different types of wave paddles. Here k_j is the j'th solution to

$$\omega^2 = gk_j \tanh k_j h \tag{3}$$

which is the linear dispersion relation generalized to complex wave numbers. It has one real solution, say k_0, and an infinity of purely imaginary solutions k_j, $j \geq 1$, where $ik_j > 0$.

Practical application in the time domain is made by use of the recursive digital filter

$$v_n = \sum_{k=0}^{M} a_k u_{n-k} + \sum_{k=1}^{N} b_k v_{n-k} \tag{4}$$

where the input u_n is $2\eta_I - \eta_0$ evaluated at time $t = n\Delta t$ and the output v_n is the wavemaker position, $X(n\Delta t)$. The transfer function of this recursive filter was fitted to match the transfer function F_0 over a wide frequency range by optimization of the filter coefficients (a_k, b_k) under stability constraints (see e.g. Antoniou, 1979). With these coefficients (4) provides the instantaneous paddle position for irregular as well as regular waves. The system only needs the instantaneous elevations of the desired incident-wave elevation, η_I and the elevation measured at the wave board, η_0. No a priori knowledge on the waves to be generated or absorbed is required.

3. Absorption theory – frequency-direction representation

Let $\eta_I(x, y, t)$ denote the elevation of the desired incident wave (i.e. the wave emitted from the wavemaker), let $\eta_0(y, t)$ be the elevation measured on the paddles of the wavemaker and let the position of these paddles be $X(y, t)$. Here (x, y) is a Cartesian coordinate system with $x = 0$ on the wavemaker.

In a linear representation the wave field to be absorbed or generated can be described as a superposition of a number of unidirectional monochromatic wave components. Thus, in this section active absorption is examined in the frequency domain concentrating on just one frequency and one wave propagation direction. Let A_I, A_0, and X_a be complex amplitudes and let c.c. denote the complex conjugate of the preceding term, then we have

$$X = \frac{1}{2}\left\{X_a e^{i(\omega t - k_y y)} + \text{c.c.}\right\} \tag{5}$$

$$\eta_I = \frac{1}{2}\left\{A_I e^{i(\omega t - k_x x - k_y y)} + \text{c.c.}\right\} \tag{6}$$

$$\eta_0 = \frac{1}{2}\left\{A_0 e^{i(\omega t - k_y y)} + \text{c.c.}\right\} \tag{7}$$

where (k_x, k_y) are the components of the wave number vector. Since waves impinging on the wavemaker will typically be reflections from some beach or structure their complex amplitude will be denoted A_R and their re-reflections from the wavemaker are termed A_{RR}. Thus, the waves emitted from the wavemaker are due to both the paddle motion and re-reflections:

$$A_I = iX_a e_0 + A_{RR} \tag{8}$$

Here e_0 is a frequency and direction dependent transfer function defined below and i is the imaginary unit representing a 90° phase shift. When no reflections

are present there will be no re-reflections and (8) reduces to an expression for pure wave generation. On the other hand, when pure active absorption is wanted then $A_I \equiv 0$ and thus the paddle generates progressive waves cancelling the re-reflections. The elevation measured on the paddle front includes both reflections and re-reflections as well as the waves generated by the movement of the paddle including the evanescent modes due to the mismatch between the shape of the paddle and the vertical structure of a progressive wave:

$$A_0 = iX_a \sum_{j=0}^{\infty} e_j + A_R + A_{RR} \tag{9}$$

Assuming full reflection at the wave paddle, we further have

$$A_R = A_{RR} \tag{10}$$

Eliminating (A_R, A_{RR}) from (8)–(10) and solving for X_a yields

$$X_a = (2A_I - A_0)\,F; \qquad F \equiv \frac{1}{i \sum_{j=0}^{\infty} e_j^*} \tag{11}$$

in which "*" denotes complex conjugation. This simple relation is the frequency-direction basis for the control of simultaneous generation and active absorption. For practical application this needs to be transformed to a time-space domain representation as shown in Chapter 5. The transfer functions constituting F are

$$e_j = \begin{cases} \dfrac{1}{\sqrt{1 - k_y^2/k^2}} c_0 = \dfrac{1}{\cos\theta} c_0 & \text{for } j = 0 \\ \dfrac{1}{\sqrt{1 + k_y^2/|k_j^2|}} c_j & \text{for } j = 1, 2, \ldots \end{cases} \tag{12}$$

where (k_j, c_j, e_j) are real for $j = 0$ and imaginary for $j = 1, 2, \ldots$. This is for the normal case, where $(k_y < k)$, so that e_0 corresponds to progressive waves. If $(k_y > k)$, then e_j is imaginary even for $j = 0$ and all modes are evanescent. For the two-dimensional case (11) reduces to (1). The transfer functions given by (12) do not account for spurious wave generation due to finite segment width of the directional wavemaker.

In addition to the frequency variation (11) also depends on the wave direction. Thus, the task is now to formulate this in the time domain somehow including the directional information. Our first ideas on how this could be done are still useful for illustrating the more general approach finally adopted. These ideas are given in the next chapter.

4. Basic ideas for inclusion of directional information

In this chapter the discussion is simplified by disregarding evanescent wave modes and considering monochromatic, unidirectional, oblique waves. Under these assumptions (11) reduces to

$$X_a = (2A_I - A_0)\,\frac{\cos\theta}{ic_0} \tag{13}$$

where the factor $\cos\theta$ makes the only difference from the flume case. Thus, for a known wave direction the correct time domain response can be obtained by replacing $2\eta_I - \eta_0$ by $(2\eta_I - \eta_0)\cos\theta$ in the instantaneous evaluation of the position of each paddle. Skourup (1996) used a numerical wave tank to show examples where this worked very well. However, generally θ is not known and an online determination of $\cos\theta$ is needed. Including the variation along the wavemaker in the amplitudes, (13) becomes

$$\hat{X}_a = \left(2\hat{A}_I - \hat{A}_0\right)\frac{\cos\theta}{ic_0} \tag{14}$$

where

$$(\hat{X}_a(y), \hat{A}_0(y), \hat{A}_I(y)) \equiv (X_a, A_0, A_I)e^{-ik_y y}; \qquad k_y = k\sin\theta \tag{15}$$

The idea is now to differentiate this expression in order to obtain some kind of directional variation. The n'th derivative

$$\frac{\partial^n}{\partial y^n}\left(2\hat{A}_I - \hat{A}_0\right) = (ik\sin\theta)^n\left(2\hat{A}_I - \hat{A}_0\right) \tag{16}$$

provides a directional variation in terms of $\sin^n\theta$, but since a cosine was the goal, we use the expansion

$$\cos\theta = \sum_{n=0}^{N} a_{2n}\sin^{2n}\theta \tag{17}$$

where a_{2n} are expansion coefficients and N is the order of the expansion. Using (16) and (17), we get

$$\left(2\hat{A}_I - \hat{A}_0\right)\cos\theta = \sum_{n=0}^{N}\frac{b_{2n}}{k^{2n}}\frac{\partial^{2n}}{\partial y^{2n}}\left(2\hat{A}_I - \hat{A}_0\right) \tag{18}$$

where

$$b_{2n} = (-1)^n a_{2n} \tag{19}$$

In principle (18) provides the input for the absorption system. In a time domain representation instantaneous elevations would replace the amplitudes. These elevations would then be given by their discrete values in time and in space along the wavemaker, typically with a spacing equal to the segment width of the wavemaker. A second derivative would then e.g. be evaluated by a central difference including three points: the elevation at the actual segment and at the two neighbouring segments. Generally, the evaluation of the $2n$'th derivative would involve (at least) $2n+1$ points i.e. n neighbouring points to each side.

Since we have avoided nonlinear relations (e.g. for expressing the cosine in terms of sines) the formulation is not restricted to one direction at one particular frequency. Application to irregular waves requires that the frequency dependent factors $1/k^{2n}$ are replaced by time domain recursive digital filters, approximating $1/k^{2n}$ for their frequency domain transfer function. Since $k \sim \omega$ in shallow water (and even $\sim \omega^2$ in deep water) $1/k^{2n}$ represents a low pass filter

of increasing order for increasing n. This filter just balances the amplification at high frequency caused by the differentiations in (18). For the general case of irregular waves the procedure outlined above involves a separate fitting of the coefficients b_{2n} and coefficients for the recursive filters representing $1/k^{2n}$. Furthermore, it relies on the neglect of evanescent modes and altogether it is more suited for explaining the principles than for practical application.

In conclusion to this chapter, differentiations of the elevations along the wavemaker are in principle able to provide the directional information required for active absorption of oblique waves. Since differentiation is equivalent to convolution with a set of filter weights it appears natural to formalize this in terms of a digital filter in space regarding the segmentation of the wavemaker as the spatial discretization. Since, for irregular waves, recursive filtering was already used with respect to the time variable, the general approach calls for a two-dimensional digital filter in time and space.

5. General approach to the time-space realization

We now return to the general case including the evanescent modes i.e. without a restriction to rather shallow water. Equation (11) in Chapter 3 gives a frequency-direction recipe for simultaneous generation and active absorption. Inspired by the above ideas we now take a general two-dimensional filter approach to the practical time-space realization of this recipe. The input to the system is a combination of desired and measured elevations and the output is the paddle position. Both input and output are regarded as functions of the coordinate along the wavemaker, y, and of time, t, sampled at $(n\Delta t, m\Delta y)$. The two-dimensional Fourier transform relates (t, y)-space to (ω, k_y)-space. Thus, we need to regard the target transfer function F from (11) as a function of (ω, k_y) instead of (ω, θ). From this point of view we can use a two-dimensional digital filter for practical time-space application:

$$v_{n,m} = \sum_{l=-M_2}^{M_2} \sum_{k=0}^{M_1} a_{kl} u_{n-k,m-l} + \sum_{l=-N_2}^{N_2} \sum_{k=1}^{N_1} b_{kl} v_{n-k,m-l} \tag{20}$$

Here the input $u_{n,m}$ is $2\eta_I - \eta_0$ evaluated at $(t, y) = (n\Delta t, m\Delta y)$ and the output $v_{n,m}$ is $X(n\Delta t, m\Delta y)$. Like the filter given in (4) for the flume case, this filter must be causal in time as the future is unknown. Thus, the counter k only takes non-negative values. However, this restriction does not apply in space, and thus the counter l runs through negative as well as positive values. The transfer function of this recursive filter was fitted to match the transfer function $F(\omega, k_y)$ over a wide range of frequencies and directions by optimization of the filter coefficients (a_{kl}, b_{kl}). Generally, the stability constraints for two-dimensional recursive filters are very complicated. At present, we omit the recursive element with respect to the spatial part of the filter, i.e. restricting ourselves to $N_2 = 0$ in (20). Furthermore, $M_2 = 1$ is used which means that at each time step the evaluation of the paddle position is only influenced by the signals at neighbouring segments. With our choice of $(\Delta t, \Delta y) = (0.025s, 0.5m)$ this allows information to travel with a speed of $\Delta y/\Delta t = 20m/s$ along the wavemaker. Since F is an even function of k_y, we get $a_{k,l} = a_{k,-l}$. It can be shown that by these restrictions the formulation basically contains the spatial

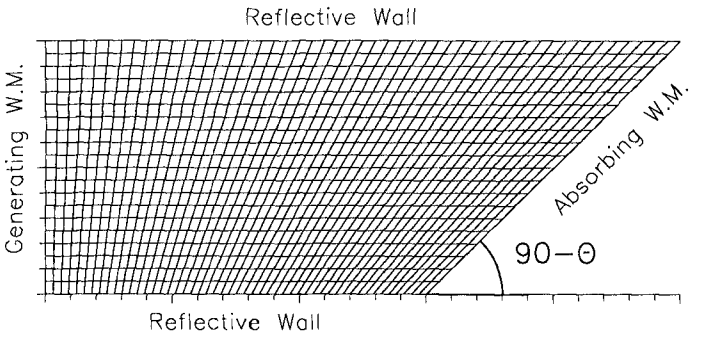

Figure 2 Top view of the numerical wave tank with a distorted rectangular grid. Wave generation at the west boundary, fully reflecting walls on the two sides and an absorbing segmented wavemaker on the oblique boundary.

derivatives from the preliminary analysis leading to (18). Only now the coefficients are found directly by fitting to the general transfer function F from (11) including evanescent-mode effects.

6. Experimental verification in a numerical wave tank

Skourup et al. (1992) developed a three-dimensional Boundary Element Model solving an integral equation for the potential flow problem in combination with an explicit time stepping procedure for updating the boundaries of the computational domain, including the free surface. Applications to a numerical wave tank equipped with a moving boundary to simulate a segmented wavemaker was described by Skourup (1996), who considered active absorption of oblique waves where the propagation direction was known a priori. In the present work this facility is used for a performance test of the 3D-AWACS as if it was a physical wave tank. However, the flexibility available in a numerical wave tank is used in the experimental setup as shown in Fig. 2. Longcrested regular waves are generated at the west boundary and propagate unaffected by the perpendicular side walls until they reach the oblique eastern boundary simulating the absorbing segmented wavemaker. The computations were made on a distorted rectangular grid fitting the boundaries. Different orientations of the oblique boundary was used to obtain a variety of different angles of wave attack relative to the absorbing wavemaker. Regular waves at two different frequencies and at angles of attack ranging from zero to 60 degrees were investigated. We first look at a frequency $f = 0.4Hz$ at which the 2D-AWACS has an almost ideal performance, cf. Fig. 1. For a wave attack of 45 degrees Fig 3 shows the instantaneous picture of the free surface after 12 periods of simulation time. Three different conditions were used on the oblique boundary to show the difference between having no absorption at all (Fig. 3a), using independent 2D-AWACS's for each

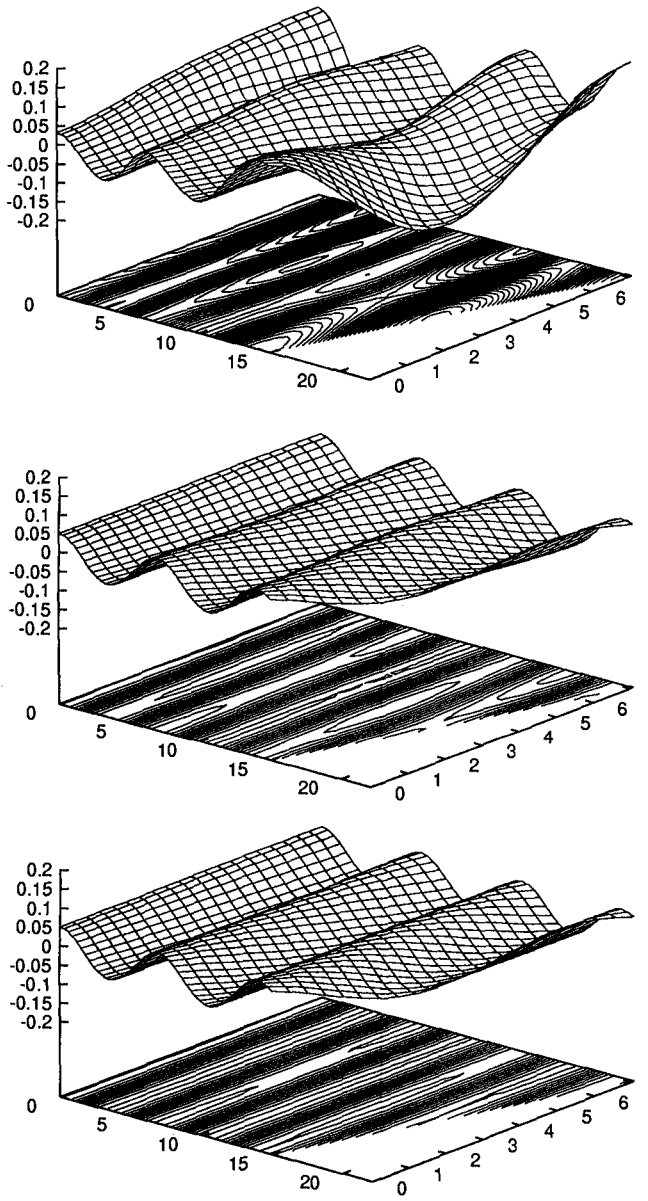

Figure 3 Waves of frequency $0.4Hz$ generated at the west boundary reflected or absorbed at the oblique boundary using a) no boundary movement b) partial absorption using 2D-AWACS c) better absorption using 3D-AWACS. Water depth 1m.

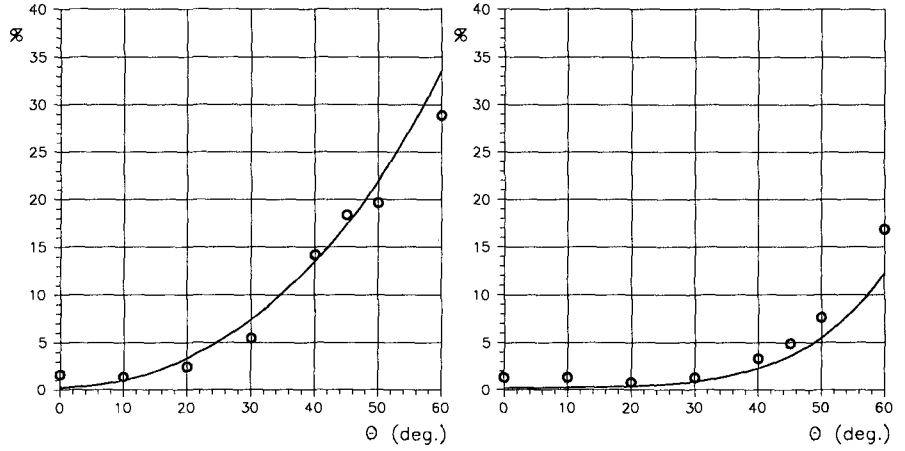

Figure 4 Reflection coefficients (%) for regular waves of frequency $0.4Hz$ versus angle of attack for a) 2D-AWACS and b) 3D-AWACS. The full curves give the theoretical performance. Water depth 1m.

segment (Fig. 3b), and using the 3D-AWACS (Fig. 3c). The pronounced cross-wave pattern for the fully reflective case (Fig. 3a) is significantly improved by use of the 2D-AWACS (Fig. 3b). Further improvement is obtained by using the 3D-AWACS.

In order to quantify the performance, time series of surface elevation and components of vertical velocity at a point in the vicinity of the absorbing wavemaker were analysed assuming the presence of three wave components: 1) One of direction θ impinging on the absorbing wavemaker 2) its (small) reflection and 3) its re-reflection from the side wall. In the postprocessing of the numerical data the angles of these three components were known and their amplitudes were calculated and used for estimation of the (small) reflection coefficients from the absorbing wavemaker. The markers on Fig. 4 show this reflection coefficient for angles θ ranging from vanishing obliqueness, $\theta = 0$ to $\theta = 60$ degrees. The performance of the 2D-AWACS is shown in Fig. 4a, while Fig. 4b gives the results for 3D-AWACS. The full curve gives the theoretical variation of the coefficient. For both systems this can be determined from the theory behind the 3D-AWACS. Again it appears that the 2D-AWACS is far better than having no absorption at all, i.e. the coefficients are small compared to 100%. The use of the 3D-AWACS further reduces the reflection to approximately one third.

The second frequency to be studied is $f = 0.7Hz$ at which the absorption coefficient of the 2D-AWACS has a local minimum, i.e. the poorest performance within a wide frequency range. Figure 5 shows the resulting reflection from the absorbing wavemaker. For the 2D-AWACS (Fig. 5a) the trend is the same as for $f = 0.4Hz$ that increasing obliqueness gives increasing reflection. However, for the 3D-AWACS, the performance is actually best around $\theta = 30$ degrees.

For these preliminary tests the aspect ratio of the boundary elements was rather high near the absorbing wavemaker in case of large θ. This gave unreliable results at $f = 0.7Hz$ and $\theta > 40$ degrees, explaining why these data do not appear in Fig. 5.

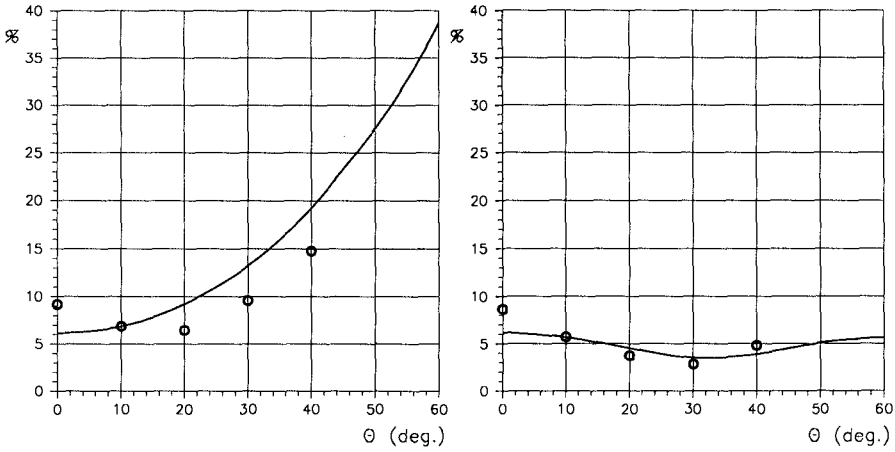

Figure 5 As Fig. 4, but for a frequency of $0.7Hz$.

7. Summary and conclusions

The development of an Active Absorption Control System for multidirectional waves called 3D-AWACS has been outlined. The theoretical basis has been derived in the frequency-direction domain and practical realization has been shown to be possible by use of a two-dimensional digital filter operating in the time-space domain, where the spatial coordinate runs along the absorbing wavemaker.

The preliminary performance of the system has been tested in a numerical wave tank including a moving boundary to simulate the segmented absorbing wavemaker. Comparative tests with a quasi three-dimensional system consisting of an array of two-dimensional absorption systems (2D-AWACS) in parallel shows that the 2D system is very much better than no active absorption and that the 3D-AWACS can further reduce spurious reflection significantly. Although the system is capable of simultaneous wave generation and active absorption, only the absorption ability was shown in these preliminary tests.

Acknowledgement. The numerical work was funded by the the Danish National Research Foundation. Their support is greatly appreciated.

Antoniou, A. (1979). Digital Filters: Analysis and Design. McGraw–Hill, New York, New York, USA.

Hirakuchi, H., R. Kajima, and T. Kawaguchi, 1990. Application of a piston–type absorbing wavemaker to irregular wave experimants. *Coastal Eng. in Japan* JSCE **33**(1), 11–24.

Hirakuchi, H., R. Kajima, T. Shimizu and M. Ikeno, 1992. Characteristics of absorbing directional wavemaker. Proc. 23rd Int. Conf. Coastal Eng., Venice Italy, 1992, ASCE, New York, 1993, 281–294.

Schäffer, H.A., 1996. Second order wavemaker theory for irregular waves. *Ocean Engng.* **23**(1), 47–88.

Schäffer, H.A., T. Stolborg and P. Hyllested, 1994. Simultaneous generation and active absorption of waves in flumes. Proc. *Waves - Physical and numerical modelling*, Vancouver, B.C., Canada, 90–99.

Skourup, J., M.J. Sterndorff and E.A. Hansen, 1992. Numerical modelling of wave-structure interaction by a three-dimensional nonlinear boundary element method: A step towards the numerical wave tank. *Ocean Engng.* **19**(5), 437–460.

Skourup, J. and H.A. Schäffer, 1995. Active absorption in boundary element modelling of nonlinear water waves. Proc. 3rd Int. Congr. on Indust. and Appl. Maths. (ICIAM), Hamburg, Germany.

Skourup, J., 1996. Active absorption in a numerical wave tank. Proc. 6th Int. Offshore and Polar Engrg. Conf. (ISOPE), Los Angeles, USA, May, 31–38.